

NN Scattering and Nucleon Quark Core

Y Yan^{a,*} and R Tegen^b

^a School of Physics, Suranaree University of Technology, Nakhon Ratchasima 30000, Thailand.

^b Permanent address: Nuclear and Particle Theory Group, Physics Department, University of the Witwatersrand, P.O. WITS, Johannesburg 2050, South Africa.

e-mail: tege@physnet,phys,wits.ac.za

* Corresponding author, E-mail: yupeng@ccs.sut.ac.th

Received 8 Feb 2000

Accepted 25 May 2001

ABSTRACT We review here nucleon-nucleon elastic and charge exchange scattering with special emphasis on the quark hard core inside the nucleon. It is found that total cross sections are sensitive only to the total hadronic size of the proton, which has two components, the quark core and the surrounding meson cloud. At higher energies differential cross sections are found to reveal, for larger $-t$, a hard core size of order ~ 0.3 fm. We present model calculations for unpolarized cross sections and find that a meson exchange model with QCD vertex functions reflecting the quark/antiquark structure of the nucleon is well capable of reproducing existing data. A quark core size of order 0.3 fm is found in our model and a preference for certain meson exchanges. As expected the pion exchange supplemented with ω , ρ , f_0 , f_2 , a_2 dominates the t -dependence of the elastic cross sections while isovector exchanges π , ρ , a_2 with a background field dominate the charge exchange n - p reaction.

KEYWORDS: Quark core of nucleon, meson cloud, nucleon-nucleon scattering, meson exchange.

INTRODUCTION

Up until the early 1920s the investigation of all matter revealed atoms as the only building blocks of matter. Soon afterwards the supposedly point-like atoms turned out to be composed of a positively charged nucleus in its center and a negatively charged electron cloud surrounding it. While the electron has so far revealed no internal structure^a the nucleus has turned out to be a rather complex particle, consisting of strongly interacting sub-particles, called "hadrons" (proton, neutron, pion, and their flavour excitations, comprising some 250 known particles).¹ All these hadrons have a finite size, of order 1 fm = 10^{-15} m, much smaller than the size of the atoms which is of order $1 \text{ \AA} = 10^{-10} \text{ m} = 10^5 \text{ fm}$. This implies that the space occupied by atoms is almost completely devoid of matter.² We will deal here with the lightest atom, the hydrogen atom H. The nucleus of the hydrogen atom H is known as the proton p ($\equiv H^+$) which is ≈ 2000 times heavier than the electron e orbiting around the proton. The sum of their charges is exactly zero, $|q_p + q_e|/e < 1.0 \times 10^{-21}$. The electrical neutrality of the hydrogen atom H is one of the experimentally best-known cosmological parameters.¹ We have recently pointed out² that the vastly different size of atoms and nuclei finds an

explanation in the mass hierarchy of the electron, pion and nucleon and in the hierarchy of the fundamental coupling constants of the electromagnetic interactions (represented by the fine structure constant $\alpha \sim 1/137$) and of the strong interactions (represented by the pion-nucleon coupling constant $g_{\pi NN} \approx 13$). Experiments done by Rutherford and, later, Hofstadter allowed to extract from the differential cross sections electromagnetic radii $\langle r_{E,M}^2 \rangle_{p,n}$, magnetic moments and more electromagnetic properties (embedded in the so-called electromagnetic form factors $G_{E,M}^{p,n}(q^2)$). Those electromagnetic radii were typically 0.8 fm (the case of the electric form factor of the neutral partner of the proton, the slightly heavier neutron, is to be treated differently, see discussion in Ref 3, 4). It turned out, however, that the size of any object (here the proton) depends on the nature of the (point-like) probe which is used in the scattering process. Electromagnetic radii are extracted by using an electron beam which interacts with the proton via the exchange of a photon γ (quantum of electromagnetic radiation). Axial radii result from neutrino beams which interact via the exchange of a W^\pm gauge boson (a heavy "partner" of the γ in the electro-weak gauge theory, see discussion in Ref 5). One finds

^a For upper limits on the electron size, see Ref 1.

$\langle r_A^2 \rangle^{\frac{1}{2}} \sim 0.5$ fm much smaller than any of the electromagnetic radii. In an analogous fashion a scalar radius of the nucleon can be defined, although not *directly* accessible to experiment.³ A typical result is $\langle r_s^2 \rangle^{\frac{1}{2}} \sim 1.2$ fm. A careful theoretical analysis of those data has revealed that, in principle, two “components” of the nucleon contribute to its size: the 3-quark core and the meson cloud surrounding it. In the electromagnetic radii both components are present while the axial radius is dominated by the 3-quark core.^{3,6} The size of this quark core is expected to be smaller than 0.5 fm. The relatively large experimental uncertainty in $\langle r_A^2 \rangle$ (due to a weak interaction process with a participating almost invisible neutrino)⁶ does not allow to pin down the size of that quark core. Some theoretical models favour a large quark core, others a small one. But how small could it really be? Topological soliton models of the nucleon represent one of the extremes. They build a nucleon out of an infinitely complex meson cloud without *any* quarks. The original MIT bag model treated the meson cloud as a perturbation thus favouring a *large* quark core. In order to decide this important question one can try to experimentally push for better neutrino scattering experiments or (and this is at first sight rather surprising) look at a more complicated scattering process under restrictive kinematical conditions. The latter approach was pursued, for different reasons, by the “high-energy” community and their results went unnoticed for a long time by the medium-energy physics community [which is interested in the low-energy (ie non-perturbative) properties of the nucleon]. From Fig 1 it is obvious that scattering of *point-like* particles (here the electron) off the extended hadron (here the proton) leads to a simpler sub-process because the known electron-photon vertex (accurately described by the well-tested gauge theory Quantum Electrodynamics, QED) can be separated off. This is not so for the proton-proton scattering process where (i) more than a photon can be exchanged and (ii) any exchanged photon etc can be exchanged between any of the 3 quarks in either of the two protons. In view of this obvious complication it came as a surprise when Povh and Hüfner⁷ were able to extract hadronic sizes for many particles, $p, \pi, K, \phi, J/\psi, \Lambda, \Sigma, \Xi, \bar{p}$ from known hadron-proton scattering data at cms^b energies beyond 15 GeV^c using the *eikonal* approximation which leads to a geometric factorisation of hadron-proton total cross sections. The emerging

pattern for the hadronic size of those elementary particles is strikingly similar to the one obtained from electromagnetic probes and in some cases is the only empirical information on the hadron’s size. Summarizing one can say that the analysis of total hadron-proton cross sections gives at a qualitative level the systematics of hadron radii and, by introducing “effective radii”, allows for a quasi-geometrical picture.⁷ Here we want to push such an approach even further in order to probe even deeper into the interior of the proton. We will refer here to high-energy nucleon-nucleon (elastic $pp \rightarrow pp$ and charge exchange (CEX) $np \rightarrow pn$) scattering, both polarised and unpolarised. Our aim is to demonstrate in this communication that pp elastic scattering becomes relatively simple at high energies and (including spin effects) is sensitive for large 4-momentum transfers to the above mentioned intrinsic 3-quark core size of the proton. This provides for a long-awaited alternative to the scarce axial form factor data from neutrino experiments.

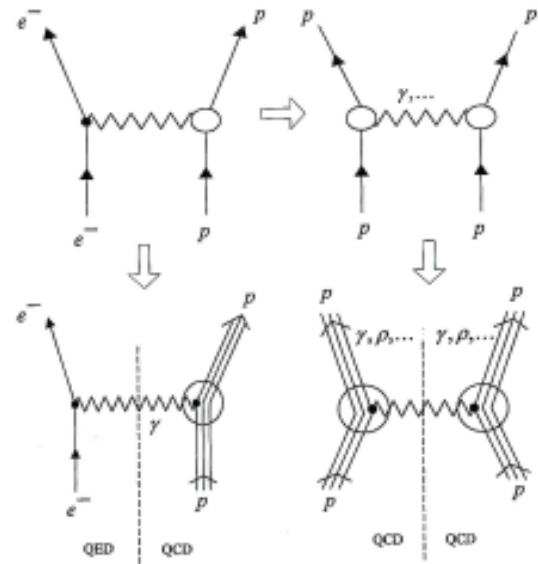


Fig 1. Feynman diagrams depicting electron-proton elastic scattering as compared to proton-proton elastic scattering. Also shown are the fundamental quark line diagrams corresponding with those processes. QED is the relativistic, quantized version of classical electrodynamics; QCD refers to the relativistic, quantized version of the nuclear (or strong) force.

^b cms stands for center-of-mass system; in this system the vectorial sum of the two incoming 3-momenta is zero -- a head-on collision, in other words.

^c This energy scale 1 GeV = 10^9 eV is to be compared with the energy equivalent of the hydrogen atoms rest mass which is ~ 940 MeV = 0.9410^9 eV and could perhaps also be compared with the electrons binding energy, -13.6 eV, in the hydrogen atom.

PROTON-PROTON SCATTERING AT HIGH ENERGIES

The elastic $pp \rightarrow pp$ reaction is an important part of the total^d $pp \rightarrow X$ reaction. In order to understand the physics behind $pp \rightarrow X$ better it is instructive to compare it with the reactions $p\bar{p} \rightarrow X$ and $e^+e^- \rightarrow X$. In Fig 2 we display total and elastic cross sections for pp and $p\bar{p}$. In theoretical models of these reactions one obtains the real part of the $p\bar{p}$ potentials by a symmetry transformation from the pp potentials (which latter are well-tested in various phase shift analyses of the nuclear potential, with low energy properties of nuclear physics, like nuclear matter density, deuteron properties, etc, as input). The imaginary part of the potential (representing the absorption /annihilation for $p\bar{p}$) is present from the start in $p\bar{p}$ as is visible in Fig 2b. In pp , however, the

inelastic channels (ie those reactions where at least one more particle appears in the final state) open up only beyond $P_{beam} = 1 \text{ GeV}/c$. The optical theorem relates the total cross-section to the imaginary part of the forward scattering amplitude

$$\sigma_{tot} = \frac{4\pi}{k} \text{Im} f(k, 0) \quad (1)$$

This relation lead to the formulation of “optical” or “diffraction” models in which inelastic processes dominate. For example the differential cross section for the elastic scattering of hadrons 1 and 2 is given at high energies as^e

$$\frac{d\sigma_{12}^{el}}{dt} \sim [n_1 g_1 G_1(t)]^2 [n_2 g_2 G_2(t)]^2 \left(\frac{s}{s_0}\right)^{2\alpha_p(t)-2} \quad (2)$$

where n_i can be related to the number of constituent quarks or antiquarks in hadron i , g_i is the Pomeron coupling to hadron i and $G_i(t)$ is the Pomeron-hadron vertex function. The Pomeron Regge trajectory is $\alpha_p(t) = \alpha_p(0) + \alpha'(t - m_p^2)$ with $\alpha_p(0) = 0$ the spin of the Pomeron and $\alpha' \sim 1 \text{ GeV}^{-2}$ the universal Regge slope. Several remarks are in order here:

- (i) Eq (2) gives the same energy dependence $s^{2\alpha_p-2}$ irrespective of the nature of hadrons 1 or 2;
- (ii) the same s -dependence dominates high-energy *total* cross sections -- this is the Pomernchuk theorem;
- (iii) the vertex functions (also called form factors) $G_i(t)$ contain the hadron's size parameter

$$\langle r^2 \rangle \equiv -6 \frac{d}{dt} G_i(t) \Big|_{t \rightarrow 0^-} \quad (3)$$

as probed by the Pomeron -- recall here our earlier remarks on the dependence of the size parameter on the probing current. The Pomeron is a hypothetical scalar particle (with vacuum quantum numbers), giving rise to a scalar radius ($\sim 1.2 \text{ fm}$, see above) while a different exchange particle like the photon γ would lead to an electromagnetic radius

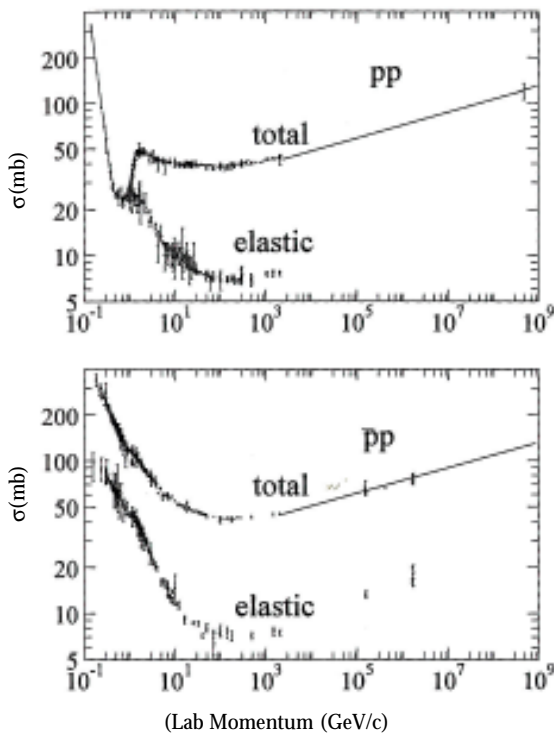


Fig 2. Plots of cross sections, in mb, versus beam momentum, in GeV/c: (a) proton proton total and elastic cross sections; (b) proton-antiproton total and elastic cross sections. Data are taken from the compilation of Ref.1.

^d Here X can be any final state compatible with known conservation laws; for example $p\bar{p} \rightarrow X$ would have X a mesonic state like $X = \pi\pi, K\bar{K}, n\bar{n}$... where as $pp \rightarrow X$ require X to have two baryons plus any number of mesons and photons, for example $X = pp, pp\pi, pp\gamma, nn + \text{lepton/ antilepton}$, ...

^e For a definition of the kinematical variables s, t, u and p_{\perp}^2 (see later), see Fig 3. Obviously the form, eq (2) is an oversimplification and (particularly at lower energies) would be expected to be more complicated for a vector meson exchange; in that case 2 instead of 1 form factors would appear in either of the square brackets of eq (2).

-- this would be relevant only at lower energies and near $t \approx 0$; note that a constant $G_i(t)$ corresponds to a point-particle (size zero).

(iv) the geometrical picture arises if the form factors $G_i(t)$ have a simple dependence on the hadron size parameter (monopole, dipole or Gaussian dependence, see eqs (6) and (7) below).

(v) the Mandelstam variable t is related to the transverse momentum p_\perp^2 , see Fig 3, which can be related to the impact parameter b by the Heisenberg uncertainty relation.^f

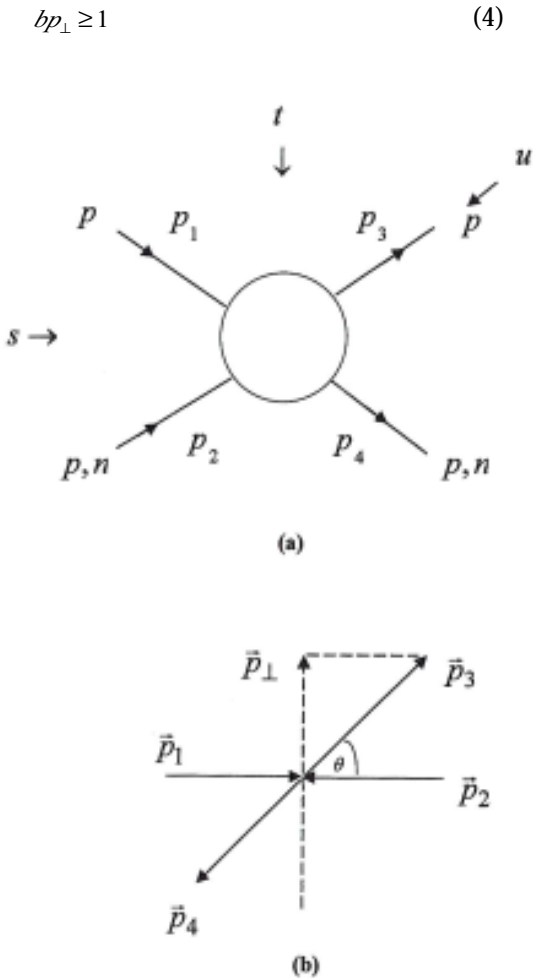


Fig 3. (a) Kinematics of a two - body reaction with the Mandelstam variables s, t and u defined in terms of 4-momenta as $s = (p_1 + p_2)^2, t = (p_1 - p_3)^2, u = (p_3 - p_2)^2$ such that $s+t+u=4m_N^2$. Scalar products refer to Minkowski space metric. The transverse momentum \vec{p}_\perp is defined in (b) in the center - of - mass system (cms). For $s \gg 4m_N^2 \approx 3.6 \text{ GeV}^2$ and $p_\perp^2 \ll s/4$ one simply finds $t = -p_\perp^2$.

see also Fig 4. Probing a size of 1/3 fm requires $p_\perp \geq 0.7 \text{ GeV}/c$ whereas a size $\frac{1}{20} \text{ fm}$ would require $p_\perp \geq 4 \text{ GeV}/c$ much larger than presently accessible by experiment. This state of affairs demonstrates a crucial dilemma in elementary particle physics. While eq (4) clearly demonstrates the need to go to higher p_\perp (or, equivalently, higher $-t$), in order to probe deeper into the interaction of hadrons or quarks/antiquarks, the differential cross sections rapidly decrease with increasing $-t$ and with increasing energy s , making experiments progressively more difficult. So, at high energies there is a clear need to reduce the unwanted background via better detectors and faster data processing.

(vi) the elastic cross sections (for both pp and $p\bar{p}$) are essentially flat between $P_{beam} = 10^2$ and $10^3 \text{ GeV}/c$. It is in this region that polarized pp scattering experiments with intriguing results have been performed.⁸

As a side-remark we mention here that the $p\bar{p}$ system has been widely studied in connection with $p\bar{p}$ bound states (atomic and deep bound states which all lie below the threshold for this reaction in Fig 2) and baryonium $B\bar{B}$ states (earlier evidence was reported between $P_{lab} = 0.4$ and $0.5 \text{ GeV}/c$ but could not be confirmed by other experiments). We recall here the somewhat simpler $e^+e^- \rightarrow X$ reaction in which the final state X has the quantum numbers of the photon and is populated by many resonances with spin = 1 and negative parity (see references 6b, 8 for a discussion of $\phi, J/\psi, \Upsilon$). The $p\bar{p} \rightarrow X$ reaction

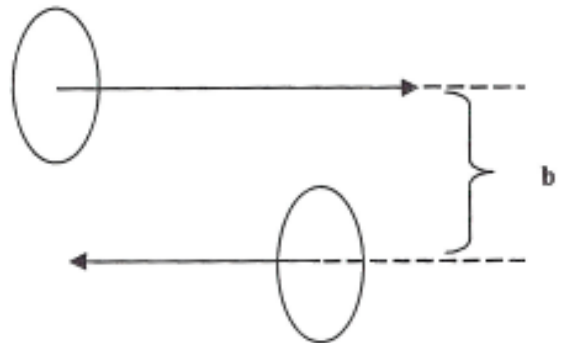


Fig 4. In the cms a collision of two extended, Lorentz - contracted hadrons is described by the impact parameter b ; the value $b = 0$ would give maximal impact (central collision) while $b \approx r$ would refer to a peripheral collision and $b > r$ would not lead to an interaction at all. r is the "radius" of the hadron in this geometrical picture. Note that this concept makes only sense for an interaction of finite range (which is the case for the nuclear (or strong) force, but is not so for the electromagnetic and gravitational interaction).

^f We use natural so that $\hbar c = 1$

involves, unlike $e^+e^- \rightarrow X$ reaction, two extended objects ($3q$ and $3\bar{q}$) annihilating via the strong interaction, see Fig 5. This seemingly unimportant fact, however, allows for many more spin-parity combinations in $p\bar{p}$ than in e^+e^- . We have recently reported¹⁰ on a whole spectrum of $p\bar{p}$ states slightly below threshold (atomic states) and between 1 and ~ 2 GeV below threshold (deeply bound $p\bar{p}$ states). Such rich structure of the $p\bar{p}$ system disappears for very high center-of-mass energies and one faces the same physics as in the pp reaction which is simpler due to the absence of the annihilation channels.

In the remainder of this communication we will therefore concentrate on the reaction $pp \rightarrow pp$ (and also the CEX $pn \rightarrow np$) and show which information

about the quark core of nucleons can be obtained by considering the high energy domain of this reaction and by including polarisation (ie spin) effects of the participating beam and target proton. Naively one would expect spin effects to be washed out as the energy is increased dramatically. Experiments at Fermilab, however, have shown that spin effects are very much alive at high energies and the resulting asymmetries (various combinations of spin-polarised differential cross sections which disappear for unpolarized cross sections) point at a ~ 0.3 fm sized quark core.

UNPOLARISED NUCLEON - NUCLEON SCATTERING

We calculate the differential cross section $d\sigma_{el}/dt$ for $pp \rightarrow pp$ and $d\sigma_{CEX}/dt$ for $np \rightarrow pn$ following standard procedures in Quantum Field Theory (see Fig 5d, 5e, and 5f). Before we present and discuss our results it is instructive to look first at phenomenological parametrisations of pertinent data. The elastic proton-proton scattering data can be parametrized as follows¹¹

$$\frac{d\sigma^{el}}{dt} = \left| A e^{-\frac{1}{2}10\rho_{\perp}^2} + \frac{B}{s} e^{-\frac{1}{2}3\rho_{\perp}^2} - C e^{-\frac{1}{2}1.5\rho_{\perp}^2} + D e^{-\frac{1}{2}0.9\rho_{\perp}^2} \right|^2 \quad (5)$$

where A, B, C, D are complex parameters and $\rho_{\perp} \sim p_{\perp}$ with an energy-dependent coefficient. The diffraction peak $e^{-10\rho_{\perp}^2}$ resulting from eq (5) is energy independent and has been interpreted in a simple, essentially non-relativistic, geometrical model as corresponding to a ~ 0.9 fm size of the proton. The

energy independent $e^{-1.5\rho_{\perp}^2}$ large $-\rho_{\perp}^2$ component in $d\sigma/dt$ would correspond in that model to a ~ 0.3 fm size in the proton while the experimentally more

uncertain $e^{-0.9\rho_{\perp}^2}$ component would indicate an ever smaller "component" inside the proton.

For the energy region considered here we take into account the following exchanges⁶: γ , $\pi(140)$, $\rho(770)$, $\omega(780)$, $f_0(980)$, $f_2(1270)$, $a_0(1320)$. The one-photon exchange produces in pp elastic cross sections the well-known "Coulomb spike" for $t \rightarrow 0$ due to the photon's spin-1 and zero rest mass. Therefore the spin-1 meson ω and ρ are also important for $t \approx 0$ while the spin-0 pion exchange contribution is more important for moderate t

First results are presented in Figs 6 and 7. The best fit to existing data gives the following set of

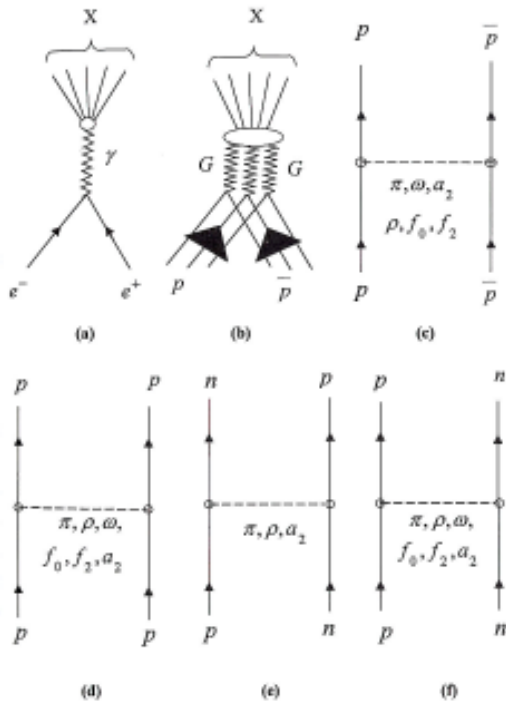


Fig 5. Feynman diagrams for various processes; time is running vertically upwards. A solid line refers to fermions (electron e^- , positron e^+ , proton p , antiproton \bar{p}) whereas a wavy line denotes a vector particle (photon γ , gluon G) and a dotted line stands for various meson exchanges (scalar, vector, tensor, as indicated). $\pi, a_0, a_2, \rho, f_0, f_2$ denote meson resonances as described in the Particle Data Group's biannual review of particle properties.¹ (a) $e^+e^- \rightarrow X$; (b) $p+\bar{p} \rightarrow X$; (c) $p+\bar{p} \rightarrow p+\bar{p}$; (d) $pp \rightarrow pp$; (e) $pn \rightarrow np$ (charge exchange); (f) $pn \rightarrow pn$ (elastic). X denotes the sum of all possible final states compatible in terms of conservation laws with the initial states in (a) - (f). The three lines in (b) refer to the 3 quarks in p and to the 3 antiquarks in \bar{p} which annihilate to form a gluon G , respectively.

⁶ The number in brackets refer to the particle's rest mass in units of MeV.

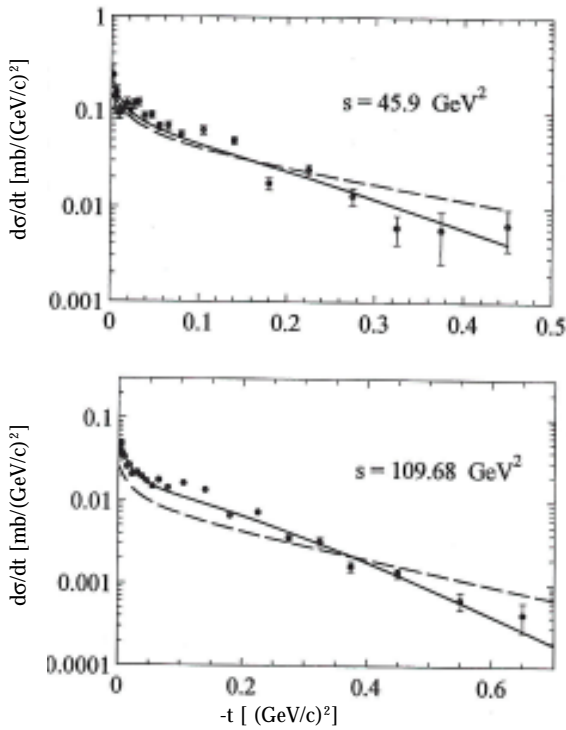


Fig 6. $d\sigma^{EX}/dt$ (shown only for $s = 45.9$ and 109.68 GeV^2) compared to experimental data (taken from the compilation of Ref. 8). Dashed curve: only π -exchange plus background field; solid curve: also ρ - and a_2 -exchange is included, see text.

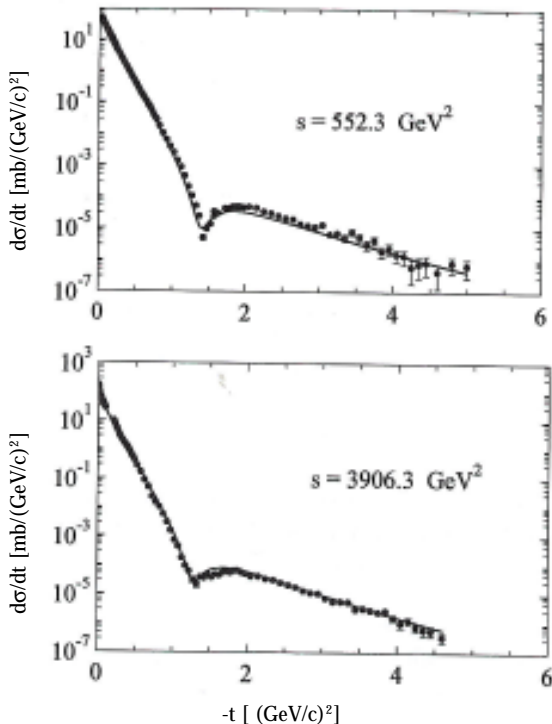


Fig 7. $d\sigma^{el}/dt$ (shown only for $s = 552.3$ and 3906.3 GeV^2) versus $-t$ Data are from the compilation of Ref 8.

coupling constants, masses and size parameters, see Table 1. The (fully relativistic) vertex functions (see the circles in Figs 5c-f) contain the desired information on the proton size. They have the analytical form

$$G(t) = G(0)e^{-t/\Lambda^2} \tag{6}$$

with $\Lambda^{-1} = \frac{1}{\sqrt{6}} < r^2 >^{\frac{1}{2}}$ the size parameter. It must

be noted here that the exponential form in eq (6) is clearly favoured by the set of data included in our analysis. A dipole fit ($n = 2, \Lambda^2 = 0.71 \text{ GeV}^2$)

$$G(t) = G(0) \frac{1}{[1 + t/\Lambda^2]^n} \tag{7}$$

or a monopole fit ($n = 1$) would be in contradiction to existing data. This is a very important observation as the empirical nucleon electromagnetic form factors require a dipole form. Clearly pp elastic scattering at high energies does not “see” the electromagnetic size of the proton but rather the 3-quark core size without the meson cloud. This view is supported by axial form factor data which also follow an exponential form, eq (6), rather than a dipole or monopole form, eq (7). As discussed in the Introduction this is so because the axial current is insensitive to the meson cloud around the 3-quark core and directly “sees” the extent of the 3-quark hard core of the nucleon (see also the discussion in Ref 6a). The question of how small the 3-quark hard core of the proton can be has recently received renewed attention. In Ref 11 a lower limit of 0.16 fm for the charge radius of the nucleon 3-quark core

Table 1. g is the scalar or vector couplings, and f is the ratio of the vector coupling to the tensor coupling. Λ is the cut-off in the form factors, eq (6), while m_0 is a parameter ascribed to the background field accompanying the pion.

Particle	$g^2/4\pi$	f	$\Lambda[\text{GeV}]$	$m_0[\text{MeV}]$
$\pi(140)$	4.66	--	0.70	100
$\rho(770)$	0.026	5.0	0.70	--
$\omega(780)$	2.35	--	0.70	--
$f_0(980)$	3.19	--	1.50	--
$f_2(1270)$	2.8×10^{-5}	0.70	1.50	--
$a_2(1320)$	0.018	1.40	0.70	--

has been derived. Given the empirical axial radius of the nucleon this puts the 3-quark (“hard”) core radius at

$$0.16 \text{ fm} \leq \langle r^2 \rangle_{quark}^{\frac{1}{2}} \leq 0.5 \text{ fm} \quad (8)$$

It is appropriate to comment here on the lower limit in eq (8). This remarkable result was obtained by using a fully relativistic valence quark model of the proton with no additional confining forces, ie only the essential spin-isospin, colour and 4-momentum correlations among the three quarks are taken into account. We would like to remark that such a model without quark confinement is not necessarily far from reality, in particular, in the high-energy domain where the total *cms* energy is much larger than any of the expected quark binding energies. This point of view is further supported by the empirically very successful Nambu-Jona-Lasinio (NJL) model of the pion (a quark-antiquark bound state in this model) which does *not* confine quarks and antiquarks, see discussion in Refs 6b, 13 and references given there to the original literature on the NJL model. It appears that the most important aspect in low energy hadron physics is the intrinsic symmetry of QCD^h and the correct implementation of its breaking pattern (in the case of the pion it is the all-important dynamical breaking of the chiral symmetry, see discussion in Ref 13). In the case of the proton the 3-quark system behaves as a spinning *rigid* body. Its parity is not a property of individual quarks anymore but a property of the 3-quark system as a whole; the projection of the total spin onto an axis, which determines the proton orientation in euclidean space, gives the parity as positive or negative. We leave the discussion of this relativistic 3-body system here and concentrate on its main result, a *lower* limit for the proton’s charge radius, see eq (8). The lowest possible value, $3/4m_N = 0.16$ fm, is obtained for a vanishing quark rest mass (highly relativistic case). For current quark masses of order 10 MeV, which are more realistic for the nucleon at hand, the corresponding radius would increase above the quoted 0.16 fm. A non-vanishing quark core size without confining forces is a purely relativistic effect known in atomic physics as the Thomas precession of electrons in an atom. In both cases the origin is the non-commutativity of successive Lorentz boosts of individual quarks/electrons (both

have spin $\frac{1}{2}$ and obey the Dirac equation, see discussion in Ref 11), which gives rise to a rotation of the spinning quarks/electrons (hence the name precession).

DISCUSSION OF UNPOLARISED RESULTS

In Fig 6 we first display our results for the *np* CEX reaction. The energy region considered here is $45.9 \text{ GeV}^2 \leq s \leq 508.4 \text{ GeV}^2$. We display here only two selected energies although the whole energy range has been used for the fits. The dashed curve shows the results with π -exchange plus a background fieldⁱ; the solid curves include ρ - and a_2 -exchange as well. The *np* CEX is very sensitive to the parameters concerning π - and ρ -exchange. The background field is important only in the CEX reaction for very small $|t|$. The background parameter m_0 as well as the parameters concerning π - and ρ -exchange are fixed by CEX data. The remaining parameters in Table 1 are fixed by comparison to the *pp* elastic data at, $552.3 \text{ GeV}^2 \leq s \leq 3906.3 \text{ GeV}^2$, see Fig 7 (only two selected energies are displayed here). Fig 6 shows that the inclusion of ρ and a_2 is important, in particular for the higher energies, as expected. It is found that it is impossible to understand the *np* data without the tensor meson a_2 . The elastic reaction, on the other hand, is insensitive to the background field, but sensitive to the parameters related to f_0 -, ω -, ρ - and f_2 -exchange. The elastic reaction is dominated by f_0 - and f_2 -exchange for $-t$ between 2 and 4 GeV^2 while the ρ - and ω -exchanges dominate the low- t peak region. The dip structure stems from the interference of the contributions of various mesons. The high- t region requires a size parameter (see Table 1)

$$\langle r^2 \rangle^{\frac{1}{2}} = \frac{\sqrt{6}}{\Lambda} = \frac{\sqrt{6}}{1.5 \text{ GeV}} = 0.32 \text{ fm} \quad (9)$$

while the low $-t$ region requires a larger size parameter

$$\langle r^2 \rangle^{\frac{1}{2}} = \frac{\sqrt{6}}{\Lambda} = \frac{\sqrt{6}}{0.7 \text{ GeV}} = 0.69 \text{ fm} \quad (10)$$

At a qualitative level we confirm the two different size parameters involved in the empirical fit to data on $d\sigma^{el}/dt$ in eq (5). Our quantitative results,

^h Quantum Chromodynamics, QCD, is the gauge theory of strong (or: nuclear) interactions, formulated in close analogy to QED.

ⁱ The concept of the background field is technically involved and we refer the interested reader to Ref 14.

eqs (9) and (10), are based on a relativistic meson-exchange model with QCD vertex functions and should give the proper dependence on any size parameter. It should be noted here that the data at higher energies do not require the asymptotic Regge form (which is expected to describe the asymptotic, ie $s \rightarrow \infty$, form of hadronic cross sections). Our observation is supported by work of other groups, see Ref 14. The prediction in eq (9) of the present work for the hard core extent of the proton is within the limits shown in eq (8).

SPIN EFFECTS IN $d\sigma^{el}/dt$ AT LARGE p_{\perp}^2

We turn now to polarisation experiments which are expected to be even more sensitive to a quark hard core (which, as we have seen in one relativistic model, is a result of the quark spin couplings in the nucleon). In the $p - p$ and $n - p$ elastic scattering experiments between 2 and 6 GeV/c the spin of the beam proton is normal to the scattering plane and may be either \uparrow or \downarrow . The target is taken as unpolarised. Note here that such an experiment for electron-proton scattering would lead to the same cross-section for \uparrow and \downarrow , see Ref 15. It is, therefore, the *strong* interaction among the spinning protons which will lead to different $d\sigma/dt$ for \uparrow and \downarrow . The analysing power is defined as

$$A = \frac{d\sigma/dt(\uparrow) - d\sigma/dt(\downarrow)}{d\sigma/dt(\uparrow) + d\sigma/dt(\downarrow)} \quad (11)$$

Simple optical models suggest $A(n - p) = A(p - p)$ while data (not shown here, see Ref 11) strongly disagree. There is clearly a need to understand the experimental $A(n - p)$ and $A(p - p)$ in a fully relativistic meson-exchange plus QCD vertex functions approach like ours. An even larger challenge to our present understanding of the proton spin distribution, as is manifest in different parametrisations of QCD vertex functions $G(t)$, see eqs (6) and (7), are elastic $p - p$ scattering data in pure initial spin states (ie both beam and target proton are polarised either \uparrow or \downarrow). For such a situation the analysing power is now defined as

$$A = \frac{d\sigma/dt(\uparrow\uparrow) - d\sigma/dt(\downarrow\downarrow)}{4 < d\sigma/dt >} \quad (12)$$

and a new observable the spin-correlation parameter, emerges

$$A_{mm} = \frac{d\sigma/dt(\uparrow\uparrow) + d\sigma/dt(\downarrow\downarrow) - 2 d\sigma/dt(\uparrow\downarrow)}{4 < d\sigma/dt >} \quad (13)$$

In naive non-relativistic quark models A in eq (12) is expected to probe the spin-orbit interaction between two 3-quark clusters; similarly A_{mm} probes the spin-spin component of that interaction as it measures the difference between the spin-parallel and spin-anti-parallel cross sections.

Data (not shown here) indicate that the spin-orbit interaction is small at large p_{\perp}^2 but important around $p_{\perp}^2 \sim 1-2 \text{ GeV}^2/c^2$, see Ref 11. The spin-spin interaction rapidly increases once p_{\perp}^2 reaches $3.6 \text{ GeV}^2/c^2$ and reaches then 30 %. This area corresponds to the interaction of the quark cores in the two interacting protons. According to eq (5) the corresponding size is in the 0.2 - 0.3 fm range, remarkably consistent with the minimal radius (8) discussed earlier.

Data indicate that the spin-parallel interaction dominates the anti-parallel interaction by a factor 2 at $p_{\perp}^2 = 4 \text{ GeV}^2/c^2$. In our model it would mean that certain meson exchanges, which are responsible for a spin non-flip at the meson-proton vertex, dominate over spin-flip meson exchanges in that particular range of p_{\perp}^2 . This is reminiscent of the low-energy analysis of Ref 16 which found that the five independent helicity amplitudes for $NN \rightarrow NN$ are dominated in forward direction (ie $t \rightarrow 0$) by different sets of meson exchanges. It will be interesting to see if such an analysis will still make sense at the much higher energies we are dealing with here.

CONCLUSION

We review here nucleon-nucleon elastic and charge exchange scattering with special emphasis on detectable evidence for a quark hard core inside the nucleon. It turns out that from center-of-mass energies of order $\sqrt{s} = 15 \text{ GeV}$ total cross sections allow to extract a hadronic size parameter comparable to the electromagnetic size of the proton $\sim 0.8 \text{ fm}$. At even higher energies and for $d\sigma/dt$ at larger transverse momenta the smaller components of order 0.2 - 0.3 fm become visible in the data. We present model calculations for unpolarized cross sections and find that a meson exchange model with vertex functions reflecting the quark/antiquark structure of the nucleon is well capable of reproducing existing

data. We find a quark core size of the expected order ~ 0.3 fm and a preference for certain meson exchanges. As expected the pion exchange supplemented with ω , ρ , f_0 , f_2 and a_2 dominates the elastic cross section while isovector exchanges π , ρ and a_2 with a background field dominate the charge exchange.

REFERENCES

1. Particle Data Group (2000) Reviews of Particle Physics. *Euro Phys J C* **15**, 1-878. (for updates visit website: <http://pdg.lbl.gov>)
2. Tegen R (2000) Why do atoms mainly consists of "empty space?". *S Afr J Sc* **96**, 515-9.
3. Tegen R (1998) Hadron radii and the origin of chiral singularities. *Acta Physica Polonica* **B29**, 3451-62; Tegen R (1998) Isovector and isoscalar meson cloud contributions to the nucleon electromagnetic form factors. *Phys Rev* **C57**, 329-44; Johnson CD, Tegen R (1999) Nucleon electromagnetic form factors and chiral singularities. *Int'l, J Mod Phys* **E8**, 1-26.
4. Kearns JP and Tegen R (1994) Charge and spin structure of protons, neutrons and pions. *S Afr J Sc* **90**, 347-53.
5. Tegen R (1995) On the mass hierarchy of fundamental particles. *S Afr J Sc* **91**, 265-70; Tegen R (1998) Die Top quark. *Die Suid-Afrikaanse Tydskrif vir Natuurwetenskap en Tegnologie* **17**, 68-71.
6. (a) Tegen R and Weise W (1983) The nucleon axial form factor and the pion-nucleon vertex function. *Z Phys* **A314**, 357-64; (b) Lemmer RH and Tegen R (1995) Meson cloud corrections to the pion electromagnetic form factor in the NJL Model. *Nucl Phys* **A593**, 315-40.
7. Povh B and Hüfner J (1987) Geometric interpretation of hadron-proton total cross sections and determination of hadronic radii. *Phys Rev Lett* **58**, 1612-5.
8. Carlson PJ, Diddens AN, Mönning F and Schopper H (1973) Nucleon-nucleon scattering. In: *Landolt-Börnstein, New Series, Group I, Vol. 7* (Edited by Schopper H), pp 5-132. Springer-Verlag; Bystricky J, Carlson P, Lechanoine C, Lehar F, Mönning F and Schubert KR (1980) Nucleon nucleon scattering. In: *Landolt-Börnstein, New Series, Group I, Vol. 9* (Edited by Schopper H), pp 7-688. Springer-Verlag.
9. Schwartz D and Tegen R (1992) Evidence for quarks. *Spectrum* **30**, 23-9; Schwartz D and Tegen R (1993) A periodic table of hadrons under the quark model. *Spectrum* **31**, 34-45.
10. Yan Y, Tegen R, Gutsche T and Faessler A (1997) Sturmian function approach and $\bar{N}N$ bound states. *Phys Rev* **C56**, 1596-604.
11. Krisch AD (1977) review talk presented at 1977 APS-DPF meeting in Argonne; (1967) Plot of all high-energy p-p scattering data using particle identity. *Phys Rev Lett* **19**, 1149-51; (1991) Precise new high measurements. *Proc 9th Int'l Symp on High Energy Spin Dynamics, Vol 1*, pp 20-33. Springer Verlag; Ramsey GP (1995) Using spin to probe hadronic structure. *Part World* **4**, 11-21.
12. de Beer W and Tegen R (1995) On the relativistic spin structure of the proton. *S Afr J Sc* **91**, 344-9.
13. Dmitrasinovic D et al. (1995) Pion and Quark electromagnetic self-masses in the NJL model. *Phys Rev* **D52**, 2855-3877; (1995) Chirally symmetric corrections to the NJL model. *Ann Phys (N.Y.)*, 332-69; (1992) Electromagnetic mass difference of the pion in the Nambu-and Jona-Lasinio model. *Phys Lett* **B284**, 201-4; (1992) The pion mass difference in the Nambu- Jona-Lasinio Model. *Comments Nucl Part Phys* **21**, 71-99.
14. Diu B and LeaderE (1975) Neutron-proton charge exchange at high energies. *Nuov Cim* **A28**, 137-54.
15. Freedom BM and Tegen R (1987) Nucleon electromagnetic form factors from scattering of polarized muons or electrons. *Phys Rev* **C36**, 2466 -72.
16. Mizutani T, Myhrer F and Tegen R (1985) Meson exchange models for low energy nucleon-antinucleon scattering. *Phys Rev* **D32**, 1663-71; Myhrer F, Mizutani T and Tegen R (1986) Low energy p bar p scattering and the quark confinement radius. *Phys Lett* **182B**, 6-10; Tegen R, Myhrer F and Mizutani T (1985) Nucleon-antinucleon annihilation via confined quark-gluon states. *Phys Rev* **D32**, 1672-1680.